

Convective Heat Transfer of Al_2O_3 and CuO Nanofluids Using Various Mixtures of Water-Ethylene Glycol as Base Fluids

Karima Boukerma

Department of Physics
 Faculty of Science, University of
 20 Août 1955 Skikda, Algeria
 phy_karima@yahoo.fr

Mahfoud Kadja

Department of Mechanical Engineering
 University of Constantine 1
 Constantine, Algeria
 kadja_mahfoud@yahoo.fr

Abstract—In this work, a numerical study has been performed on the convective heat transfer of Al_2O_3 /Water-Ethylene Glycol (EG) and $\text{CuO}/(\text{W}-\text{EG})$ nanofluids flowing through a circular tube with circumferentially non-uniform heating (constant heat flux) under the laminar flow condition. We focus on the study of the effect of EG-water mixtures as base fluids with mass concentration ranging from 0% up to 100% ethylene glycol on forced convection. The effect on the flow and the convective heat transfer behavior of nanoparticle types, their volume fractions ($\phi=1\text{-}5\%$) and Reynolds number are also investigated. The results obtained show that the highest values of the average heat transfer coefficient is observed between 40% and 50% of EG concentration. The average Nusselt number increases with the increase in EG concentration in the base fluid, and the increase in the Reynolds number and volume fraction. For concentrations of EG above 60%, and for all volume fractions, the increase of thermal performance of nanofluids became inversely proportional to the increase of Reynolds number. In addition, $\text{CuO}/(\text{W}-\text{EG})$ nanofluids show the best thermal performance compared with Al_2O_3 /(W-EG) nanofluids.

Keywords-enhanced heat transfer; nanofluids; numerical study; concentration; performance index

NOMENCLATURE

C_p	specific heat, $\text{J kg}^{-1} \text{K}^{-1}$
D	tube diameter, m
d	nanoparticle diameter, m
h	heat transfer coefficient, $\text{W m}^{-2} \text{K}^{-1}$
k	thermal conductivity, $\text{W} \cdot \text{m}^{-1} \cdot \text{K}^{-1}$
L	length of the tube, m
Nu	Nusselt number
P	Pressure, pa
q_w	uniform heat flux, W m^{-2}
Re	Reynolds number ($\rho w_{in}D/\mu$)
r	radial direction
T	temperature, K
u	tangential velocity, m s^{-1}
v	radial velocity, m s^{-1}
w	axial velocity, m s^{-1}

Z axial direction

Greek symbols

ΔP	pressure drop, Pa
θ	angular coordinate
μ	Viscosity, $\text{kg m}^{-1} \text{s}^{-1}$
ϕ	volume fraction
ψ	volume fraction of mixture
ρ	density, kg m^{-3}
κ	Boltzmann constant, $1.381 \times 10^{-23}, \text{J K}^{-1}$

Subscripts

ave	average
b	bulk
bf	base fluid
in	inlet
nf	nanofluid
p	nanoparticle
w	wall

I. INTRODUCTION

The efforts to enhance the heat exchangers performance in many industrial sectors (automotive, electronics, etc.) require the intensification of heat transfer by convection. Improvements in exchange surfaces are a pathway already widely explored and reach their limits [1]. New optimization pathways must be considered. One of them is to use new fluids able to increase heat transfer such as the nanofluids. The nanofluids are nano-sized particle dispersions in a base fluid in order to improve certain properties. The diameter of such particles (called nanoparticles) is typically less than 100 nm [2]. In the case of a cooling liquid, one of the leading parameters to be taken into account to evaluate the potential for heat exchange is the thermal conductivity. However, the most widely used fluids, such as water, ethylene glycol (EG) or oil have only a low thermal conductivity relative to that of the solid. With nanofluids, the idea is to insert the nanoparticles in a base fluid in order to increase the effective thermal conductivity of the mixture.

In [3], authors studied the nanofluids by preparing a mix of 100 nm of Cu nanoparticles with water and oil. They found that

the thermal conductivity of nanofluids increases considerably with the concentration of nanoparticles. Then they proposed a correlation to calculate the Nusselt number as a function of Peclet number for nanofluids. In [4], authors experimentally studied the forced convection laminar flow of CuO/water and Al₂O₃/water nanofluids in a tube under constant temperature. They indicated that there is an increase in heat transfer with an increase in volume concentration for both nanofluids, but they found that Al₂O₃ nanoparticles are more performant. In [5], authors studied a two dimensional laminar flow inside a triangular duct with the existence of a vortex generator. Three types of nanofluids (Al₂O₃/EG, CuO/EG and SiO₂/EG) with volume concentrations ranging from 1 to 6% were considered. Their results show that SiO₂/EG has the highest value of Nusselt number compared to other nanofluids. On the other hand, the value of the friction coefficient is the same for all nanofluids and nanoparticles concentrations considered.

Due to its relatively low molecular weight, ethylene glycol greatly lowers the water freezing point. Therefore, the mixture of water–ethylene glycol was often used in cold countries [6-7]. Several researchers measured experimentally the rheological properties of nanofluids with an EG-water mixture base fluid [8-10], and they proposed correlation equations for the thermophysical properties such as: viscosity, thermal conductivity and specific heat [11-12]. These properties were used to develop correlations for Nusselt number and/or friction factor from experiments, as a function of these properties and the nanoparticle volume concentrations [13-15]. In [16], authors conducted an experimental study on the forced convective heat transfer of TiO₂ nanoparticles with mixture of EG-water (40:60 by volume) in a copper tube under laminar conditions. Moreover, they studied the effect of mixtures of water and EG base fluid with different volume fractions (ranging from 0 % up to 50 % ethylene glycol) on local Nusselt number. They found that there is 8.25 –20.52% increase in Nusselt number when the EG fraction in water increases from 0 to 50%. In [17], authors measured the heat transfer coefficient of the secondary refrigerant based CNT (carbon nanotubes) nanofluid in a tubular heat exchanger at different operating temperatures. The base fluid was a mixture of EG -water (30:70 by volume). The obtained results showed that at 40 °C with a 0.45 Vol. % CNT nanofluid the increase in thermal conductivity and average convective heat transfer coefficient was 19.73% and 159.3% respectively. They concluded that such increases occur because of the micro convection effects of the chaotic movement of the carbon nanotubes. In another study [18] with the same nanofluid cited above they investigated the convective heat transfer in various lengths of a tubular heat exchanger. They reported that contrary to what is customary for heat transfer, the Nusselt number decreases with an increase in the Reynolds number as the MWCNT (multiwalled carbon nanotubes) concentration increases in the base fluid.

Most of the articles, which dealt with the experimental or numerical research on heat transfer and nanofluid flow with an EG-water mixtures base fluid, are for fixed EG fractions in water and only a few considered different volume fractions, but in maximum up to 50%. This research focuses on the study of the effect of ethylene glycol based Al₂O₃ and CuO nanofluids

on forced convection in a circular tube with circumferentially non-uniform heating. The EG-water mixtures used in the computations have EG mass concentrations which vary in the interval from 0% up to 100 %. Heat transfer with circumferentially non-uniform heating occurs in many applications such as evaporators, boilers and solar collectors [1].

II. NUMERICAL SIMULATION

A. Geometry

In this study, we considered laminar forced convection flow of a nanofluid in a straight cylindrical pipe with a diameter D of 0.01m and the length L of 1m. The length was chosen so as to obtain hydrodynamically and thermally fully-developed flow at the outlet section. The tube was heated on one side (upper half) with a constant heat flux and insulated over the lower side. The problem treated is shown schematically in Figure 1.

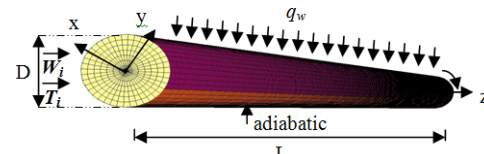


Fig. 1. Geometry and boundary conditions

B. Governing equations

Our problem is modelled as laminar, steady flow and the three-dimensional one phase model for the nanofluid was used. Pressure work and dissipation are neglected. The thermophysical properties of the nanofluid are assumed to be constant. Under these assumptions the governing mass, momentum and energy equations for the nanofluid can be written as follows:

Continuity equation:

$$\nabla \cdot (\rho_{nf} \vec{V}) = 0 \quad (1)$$

Momentum equations:

$$\nabla \cdot (\rho_{nf} \vec{V} \vec{V}) = -\nabla P + \nabla \cdot (\mu_{nf} \nabla \vec{V}) \quad (2)$$

Energy equation:

$$\nabla \cdot ((\rho C_p)_{nf} \vec{V} T) = \nabla \cdot (k_{nf} \nabla T) \quad (3)$$

C. Boundary conditions

The nanofluid enters the channel at the inlet with a uniform axial velocity that is specified according to the flow Reynolds number. The inlet temperature T_{in} is taken as 300 K. The no-slip boundary conditions at the walls are implemented in the present study, and a constant heat flux (5 kW/m²) is applied through the top half of the tube, while the bottom wall is considered adiabatic. For the channel outlet, the fully developed flow boundary condition is adopted. The boundary conditions can therefore be expressed as:

- At the inlet of tube (z=0):

$$w=w_{in}, \quad u=v=0 \quad \text{and} \quad T=T_{in} \quad (4)$$

- At the fluid-wall interface ($r=D/2$):

$$u=v=w=0 \quad (5)$$

$$0 \leq \theta \leq \pi : -k_{nf} \frac{\partial T_{nf}}{\partial r} = q_w \quad (6)$$

$$\pi \leq \theta \leq 2\pi : -k_{nf} \frac{\partial T_{nf}}{\partial r} = 0 \quad (7)$$

- At the tube outlet ($z=L$): the outflow boundary condition is applied, in which the flow velocity and temperature profiles are unchanging in the flow direction.

C. Thermophysical properties

The base fluid is a mixture of water and EG in different mass concentrations, their thermophysical properties are calculated as follows [19]:

$$\zeta_m = \psi \zeta_{EG} + (1-\psi) \zeta_{Water} \quad (8)$$

Where m refers to "mixture", ψ is the volume fraction of the mixture and ζ is the fluid physical property, for example: density, specific heat, thermal conductivity and viscosity. The thermophysical properties of the mixture are greatly modified by the addition of nanoparticles. Many parameters characterizing these nanoparticles can have a significant effect on the values of the thermophysical parameters of the nanofluid obtained (the volume fraction φ , the size of the nanoparticles, the thermal conductivity of the base fluid and that of the nanoparticles, the temperature of the medium, etc.). The thermophysical properties of water, Ethylene Glycol (EG), Al_2O_3 and CuO are summarized in Table I. In this work, we assume that the nanoparticles are well dispersed in the base fluid. In order to calculate the thermophysical properties of the nanofluid, we use the equations given below which were found in the literature. In [9], author compared their density measurements of different nanoparticles in a base fluid of 60:40 ethylene glycol/water with predictions using equation (9) which was proposed in [20], and they found an excellent agreement between them.

$$\rho_{nf} = (1-\varphi)\rho_{bf} + \varphi\rho_p \quad (9)$$

Where ρ_{nf} , ρ_{bf} and ρ_p are the nanofluid, base fluid and nanoparticles densities, respectively, and φ is the volume fraction.

The specific heat of nanofluids C_{pnf} is computed using Xuan and Roetzel's equation [21].

$$C_{pnf} = \frac{(1-\varphi)\rho_{bf} C_{pbf} + \varphi\rho_p C_{pp}}{\rho_{nf}} \quad (10)$$

Where C_{pbf} and C_{pp} are specific heat at constant pressure of the base fluid and nanoparticles, respectively.

The thermal conductivity formula proposed by Vajjha and Das [8] was used in this study. It incorporates the classical Maxwell model and the Brownian motion effect and is given by:

$$k_{nf} = \frac{k_p + 2k_{bf} - 2(k_{bf} - k_p)\varphi}{k_p + 2k_{bf} + (k_{bf} - k_p)\varphi} k_{bf} + 5 \times 10^4 \beta \varphi \rho_{bf} C_{pbf} \sqrt{\frac{\kappa T}{\rho_p d_p}} f(T, \varphi) \quad (11)$$

Where the empirical function $f(T, \varphi)$ for the nanofluids Al_2O_3 and CuO is given by:

$$f(T, \varphi) = (2.8217 \times 10^{-2}\varphi + 3.9117 \times 10^{-3}) \left(\frac{T}{T_0} \right) + (-3.0669 \times 10^{-2}\varphi - 3.91123 \times 10^{-3}) \quad (12)$$

The factor β is presented in Table II. It is found using the experimental data of [8], and it represents the fraction of the liquid volume that travels with a particle.

The viscosity of the nanofluid μ_{nf} is function of the volume fraction and viscosity of the base fluid μ_{bf} and is evaluated using the following equation [23]:

$$\mu_{nf} = A_1 e^{(A_2 \varphi)} \mu_{bf} \quad (13)$$

Where A_1 and A_2 are constants, their values are given in Table III.

TABLE I. THERMOPHYSICAL PROPERTIES OF NANOPARTICLES AND BASE FLUIDS AT $T=300$ K [22, 27]

Properties	Water	EG	Al_2O_3	CuO
Density (kg/m ³)	997	1,114.4	3,600	6,500
Thermal Conductivity (W/m K)	0.613	0.252	36	17.65
Specific Heat (J/kg K)	4179	2415	765	533
Viscosity (N/m ² s)	0.000855	0.0157	-	-

TABLE II. THE VALUES OF THE FACTOR β FOR Al_2O_3 AND CUO NANOPARTICLES.

Type of particles	β	concentration	Temperature
Al_2O_3	$8.4407(100\varphi)^{1.07304}$	$1\% \leq \varphi \leq 10\%$	$298K \leq T \leq 363K$
CuO	$9.881(100\varphi)^{0.9446}$	$1\% \leq \varphi \leq 6\%$	$298K \leq T \leq 363K$

TABLE III. VISCOSITY COEFFICIENTS FOR Al_2O_3 AND CUO NANOPARTICLES.

nanoparticles	A_1	A_2	concentration
Al_2O_3	0.983	12.959	$1\% \leq \varphi \leq 10\%$
CuO	0.9197	22.8539	$1\% \leq \varphi \leq 6\%$

III. NUMERICAL METHOD AND VALIDATION

The simulation was carried out using FLUENT. The resolution of (1)-(3) is performed by discretizing the computational domain. In this way, all the discrete points constitute the computational domain mesh. At each discrete point of the domain, FLUENT uses the finite volume method for obtaining algebraic expressions which replace the non-linear partial differential equations and which can be solved numerically. The resulting set of algebraic equations predicts the mass, momentum and energy in all the discrete points of the mesh. The finite volume method consists of integrating the conservation equations over each control volume in the mesh. The convective and viscous terms are discretized with a second order upwind scheme for more accuracy. The SIMPLE algorithm is used for pressure-velocity coupling. The convergence of the iterative process is determined by the concept of residues. In this study, the discretized equations are considered converged when all the equations have a residue less than 10^{-6} . The Gambit software was used to perform a 3D mesh. After several trials, we obtained the threshold of the

grids finesse above which the calculated solution becomes grid independent.

The simulation was carried out on three types of grids ($5 \times 32 \times 500$, $7 \times 40 \times 500$, $10 \times 64 \times 500$) for pure water. Figure 2 shows the independence test for the calculated local Nusselt number along the tube on the grids used. According to the result of this test the mesh chosen is that with an average number of discretization points equal to ($7 \times 40 \times 500$). We can also notice in Figure 2 that our numerical results are in good agreement with the correlation developed in [28]. The validation of the CFD code has also been tested using the experimental results obtained by [24]. This result concerns the laminar flow in a circular tube heated by a constant flux where the heat flux (q_w) equals to 9000 W/m^2 and the Reynolds number (Re) is about 799.53. The results for the local Nusselt number (Figure 3) agree well with our results.

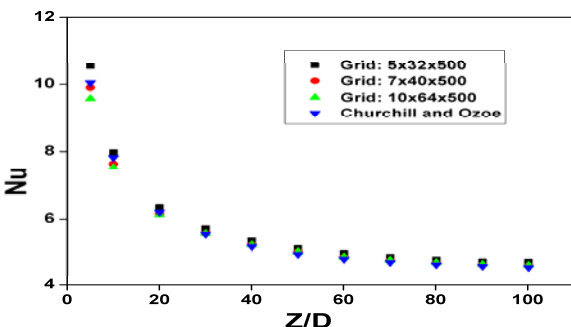


Fig. 2. Comparison of local Nusselt number values for different grids

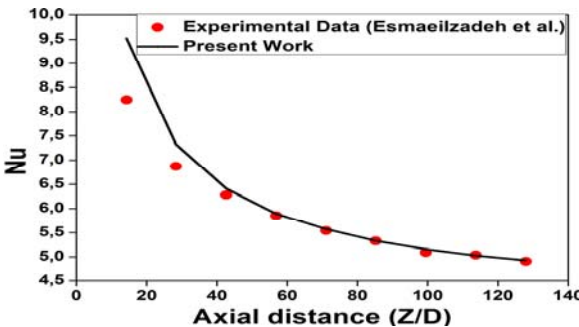


Fig. 3. Comparison of numerical local Nusselt number with the experimental values of [24]

The local Nusselt number and local heat transfer coefficient are calculated using the following equations:

$$Nu(z) = \frac{h(z) \cdot D}{k} \quad (14)$$

$$h(z) = \frac{q_w}{T(z)_w - T(z)_b} \quad (15)$$

Where D and $T(z)_w$ are the tube diameter and wall temperature respectively, and $T(z)_b$ is the bulk fluid temperature calculated as follows:

$$T(z)_b = \frac{\int_A \rho V_z T dA}{\int_A \rho V_z dA} \quad (16)$$

The average heat transfer coefficient (h_{ave}) and Nusselt number are expressed as [25]:

$$h_{ave} = \frac{q}{\overline{T}_w - \overline{T}_b} \quad (17)$$

$$Nu_{ave} = \frac{h_{ave} \cdot D}{k} \quad (18)$$

Where \overline{T}_w and \overline{T}_b are the wall and fluid average temperature respectively.

IV. RESULTS AND DISCUSSION

The convective heat transfer was numerically investigated for flow of Al_2O_3 and CuO nanofluids in a horizontal cylindrical tube which was heated on one side. Mixtures of Ethylene glycol/water as base fluid with mass concentration ranging from 0% to 100% ethylene glycol were used (so we get eleven base fluids). The computations were carried out with the Reynolds numbers of 250, 500, 750 and 1000, and with different volume fractions of the nanoparticles which vary from 0% to 5%. Figure 4 shows the average heat transfer coefficient (h_{ave}) of base fluid mixtures of water/EG at different Reynolds numbers. The highest values of the average heat transfer coefficient is observed between 40% and 50% of EG concentration, for instance at $Re=250$ the values are 681.3 and 683.7 ($\text{W/m}^2\text{K}$) respectively. As expected the heat transfer coefficient increases when the Reynolds number increases. At a given Reynolds number, the base fluid mixtures of water-EG (with different mass. % of EG) have highest average heat transfer coefficients, followed by ethylene glycol and pure water respectively. The effect of volume fraction ($\phi\%$) on average heat transfer coefficient for $\text{Al}_2\text{O}_3/\text{W-EG}$ nanofluids at $Re=1000$ is depicted in Figure 5.

The average heat transfer coefficient increases as the volume fraction of Al_2O_3 nanoparticles increases in the base fluid. Also we can see that the highest values of h_{ave} are between 40% and 50% of EG concentration. The influence of the Reynolds number and the volume fraction on average Nusselt number is illustrated in Figures 6 and 7. Figure 6 shows the effect of Re on the average Nusselt number (Nu_{ave}) for a low volume fraction (1%) of Al_2O_3 nanoparticles. Nu_{ave} of $\text{Al}_2\text{O}_3/(\text{water-EG})$ nanofluids is found to be higher than that of $\text{Al}_2\text{O}_3/\text{water}$ and lower than that of $\text{Al}_2\text{O}_3/\text{EG}$. The reason being that the thermal conductivity of water is greater than that of water-EG mixtures and EG, respectively. Figure 7 represents the variation of Nu_{ave} with volume fraction of $\text{CuO}/(\text{water-EG})$ nanofluids at $Re=1000$. The average Nusselt number of the nanofluids is greater than that of base fluids. Nu_{ave} increases as the concentration of ethylene glycol in the base fluid or the Reynolds number or the volume fraction increase. The enhancement of thermal performance with CuO nanofluids is higher than that with Al_2O_3 nanofluids especially at great values of Reynolds number and volume fraction.

Figure 8 shows the thermal performance of nanofluids using different concentrations of ethylene glycol in the base fluid. The curves present the results of the average heat transfer coefficient ratio (h_{nf}/h_{bf}) between the nanofluid and the base fluid (it should be noted again that each concentration of EG represents a base fluid) at different volume fractions. As can be noticed there is an increase in heat transfer ratio as the

nano particle volume fraction increases. In the case of Al_2O_3 nanoparticles and at $Re=250$ the heat transfer coefficient ratio increases with the increase of the concentration of EG in the base fluid; but for other values of Re the ratio h_{nf}/h_{bf} increases and then it decreases, for instance at $Re=500$ and 1,000 the decrease in the ratio occurs at 80% and 40% of EG, respectively. Consequently, it is observed that the increase in the ratio h_{nf}/h_{bf} is directly proportional, as expected, to the increase of the Reynolds number for concentrations situated between 0% to 20% of EG. For concentrations between 30% and 40% of EG this ratio has approximately the same value. We find that from 50% of EG the ratio h_{nf}/h_{bf} decreases with increasing Reynolds number and that this decrease appears more clearly from 80 % of EG in the base fluid.

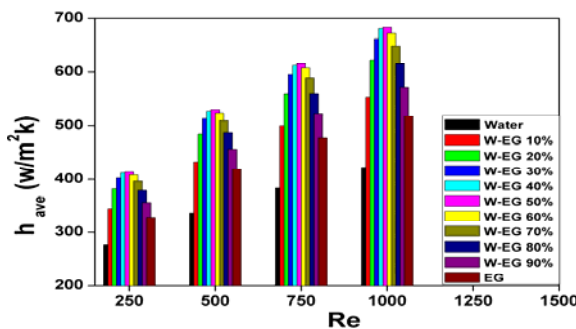


Fig. 4. Effect of Reynolds number and water-EG mixture on average heat transfer coefficient

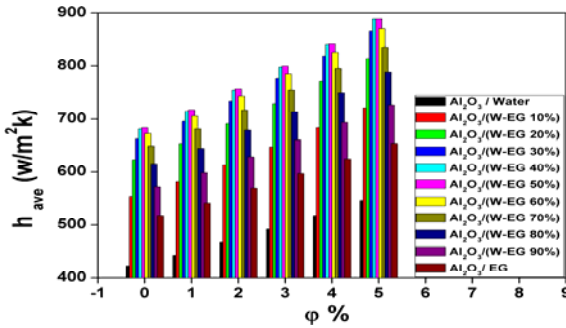


Fig. 5. Variation of average heat transfer coefficient with volume fraction for Al_2O_3 /(W-EG) nanofluids

Concerning the CuO nanoparticles, we always get the same behavior as regards the influence of the concentration of EG on the heat exchange ratio for the different Reynolds numbers. But we note that the decrease of the ratio h_{nf}/h_{bf} appears at a concentration of EG more advanced (about 30% of EG at $Re=1,000$ and $\varphi=4\%$) and in a faster manner than that of Al_2O_3 nanofluids, and the inverse proportionality occurring between the heat transfer ratio and the Reynolds number happens early at a concentration of 40% of EG in the base fluid. We can clearly observe from Figure 8 that the $\text{CuO}/(\text{W}-\text{EG})$ nanofluids have the best average heat transfer coefficient ratio (heat transfer enhancement) compared with Al_2O_3 /(W-EG) nanofluids. The inverse relationship that occurs between the convective heat transfer ratio and the Reynolds number and which increases with the volume fraction and the concentration of EG in base fluid, is probably caused by the increase in the viscosity upon the addition of nanoparticles and also because of

the high viscosity of the EG compared to water, and may be at low Reynolds numbers the increase of concentration of EG in the base fluid makes the nanoparticles more effective.

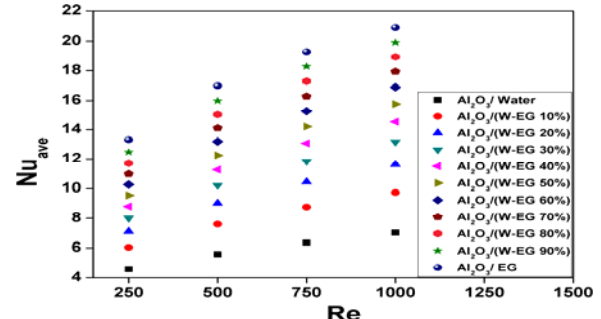


Fig. 6. Variation of Nusselt number with Reynolds number for Al_2O_3 /(W-EG) nanofluids

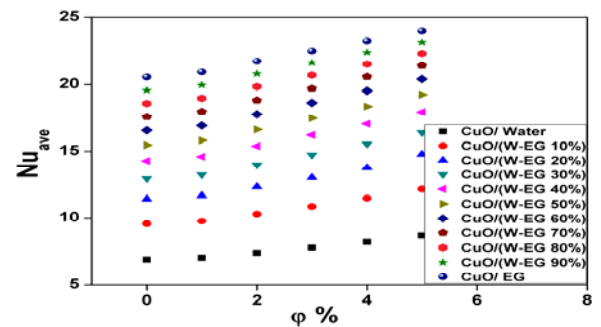


Fig. 7. Variation of Nusselt number with volume fraction for $\text{CuO}/(\text{W}-\text{EG})$ nanofluids

From the above observations the nanofluids appear to be ideal when considering an increase in the thermal performance of heat transfer equipment. The addition of nanoparticles in a fluid allows an increase of the thermal conductivity but unfortunately also the viscosity which usually leads to an increase in pressure loss in the system. In the industrial applications of nanofluids, although an improvement of heat transfer is observed, the required pump power is increased compared with the case of the conventional fluid. A significant increase in the viscosity of the nanofluid could lead to an unfavorable energy performance of the industrial system. To illustrate this, we used a performance index " η " [26], where η represents the ratio between heat transfer enhancement and pressure drop in the system:

$$\eta = \left(\frac{h_{ave,nf}}{h_{ave,bf}} \right) \left/ \left(\frac{\Delta P_{nf}}{\Delta P_{bf}} \right) \right. \quad (19)$$

Where $h_{ave,bf}$ and ΔP_{bf} are the average heat transfer coefficient and pressure drop of base fluids.

To determine the effectiveness of each nanofluid, relative to its base fluid, Figure 9 shows the variation of the performance index with Al_2O_3 /(W-EG) and CuO /(W-EG) nanofluids for various volume fractions at $Re=500$. In this case $h_{ave,bf}$ and ΔP_{bf} are the average heat transfer coefficient and pressure drop of the water-EG base fluid, respectively. As shown in this figure the performance index is below 1. So we can conclude that the base fluid (W-EG) is more effective, from the thermal point of

view, than the nanofluids. It is noted that the performance index decreases with the increase of the volume fraction of the nanoparticles, but it does not change with the concentration of EG (that is why we stopped at 50% of EG in this figure). We also see that the performance index of Al_2O_3 nanofluids is higher compared to the one of CuO nanofluids.

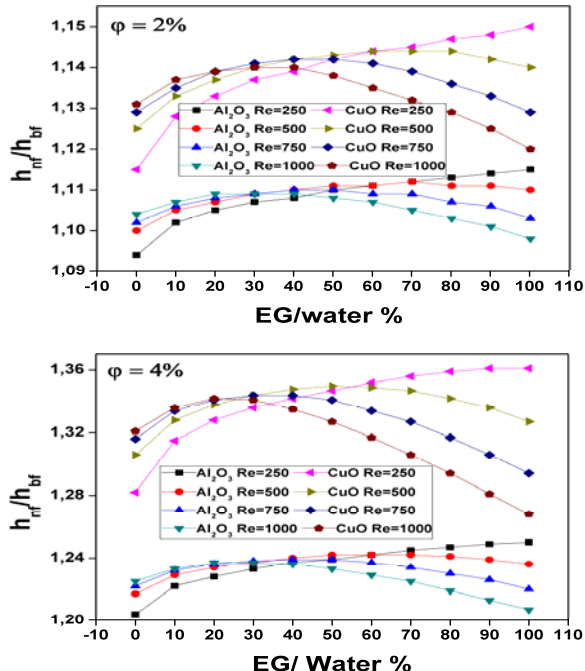


Fig. 8. Effect of different base fluids on heat transfer enhancement for various Reynolds numbers and nanoparticles.

Figure 10 shows the evolution of the performance index as a function of the Reynolds number in the case of water-EG based fluids. We can see that all the values corresponding to the base fluids (W-EG) are above those corresponding to the case of pure EG. This means that the performance index of base fluids, as it is defined, is favorable for the whole range of the concentration of EG. However, this performance index has significantly decreased with an increase of the concentration of EG in the base fluid. For example when the concentration of EG varies from 10% to 90%, η decreases from 49.36 to 1.36 for $Re=1,000$. On the other hand, there is a small change in the value of the performance index with Reynolds number.

The evolution of the performance index with Al_2O_3 /(W-EG) nanofluids for different volume fractions at $Re=500$ is depicted in Figure 11. We note that the performance index decreases when the volume fraction of nanoparticles and the concentration of EG increase. For the concentration of EG varying from 10% to 70% in the base fluid we have a performance index greater than 1, which implies the use of nanofluids is favorable than pure EG. But from 80% of EG onwards the performance index becomes less than 1 for some volume fractions. For example η is less than 1 at $\varphi=4\%$ for the concentration of 80% of EG and at $\varphi=2\%$, for the concentration of 90% of EG.

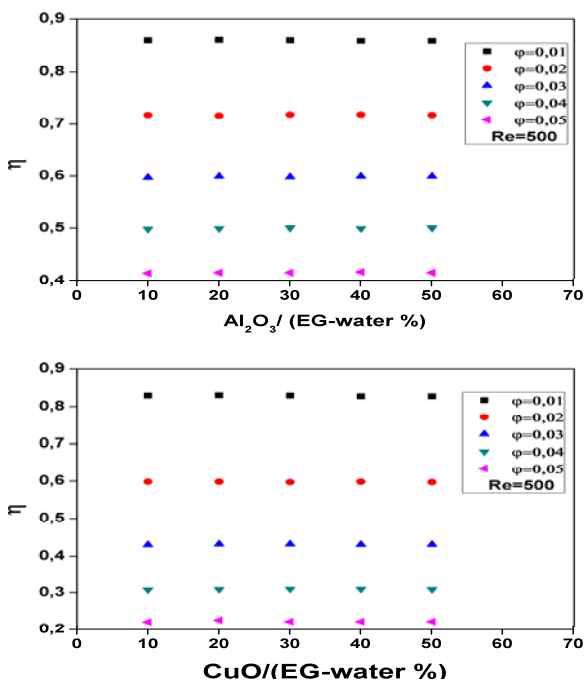


Fig. 9. Variation of the performance index for different volume fractions with Al_2O_3 /(W-EG) and CuO /(W-EG) nanofluids

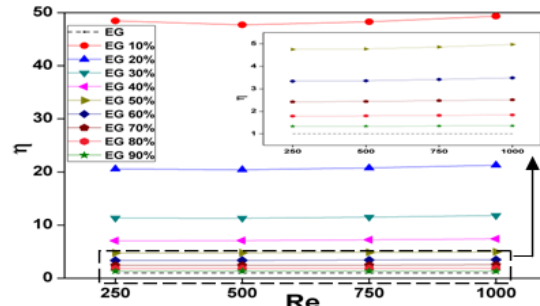


Fig. 10. Evolution of the performance index as a function of the Reynolds number for different base fluids

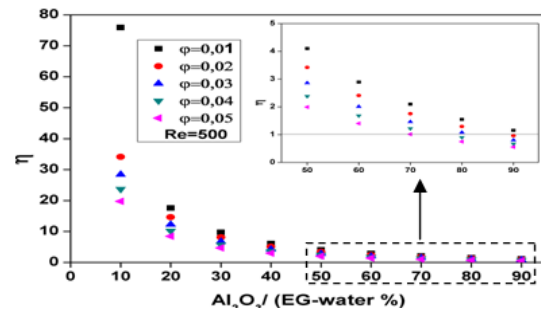


Fig. 11. Variation of the performance index with Al_2O_3 /(W-EG) nanofluids for different volume fractions.

Figure 12 shows the variation of the performance index with CuO /(W-EG) nanofluids for different volume fractions at $Re=500$. It is observed that the performance index is greater than 1 up to 50% of EG, and then begins to decrease when the volume fraction and the concentration of EG increase. For instance, η is less than 1 at $\varphi=5\%$ for the concentration of 60% of EG and at $\varphi=3\%$ for the concentration of 80% of EG.

According to the two figures, we see that the performance index is always greater than 1 for $\varphi=1\%$, and we also see that the $\text{Al}_2\text{O}_3/(\text{W-EG})$ nanofluids have the highest performance index that the $\text{CuO}/(\text{W-EG})$ nanofluids.

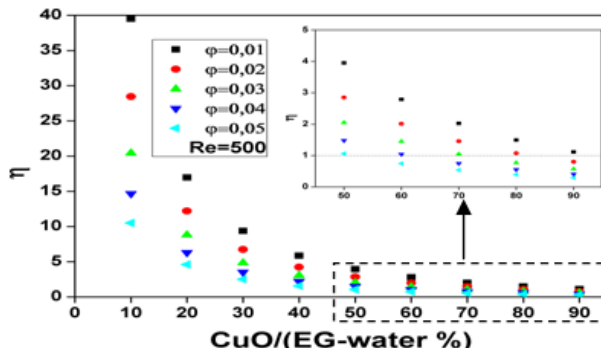


Fig. 12. Variation of the performance index with $\text{CuO}/(\text{W-EG})$ nanofluids for different volume fractions

V. CONCLUSION

We investigated in the present research the effect of water-EG based nanofluids with various compositions on convective heat transfer performance. Heat transfer due to $\text{Al}_2\text{O}_3/(\text{W-EG})$ and $\text{CuO}/(\text{W-EG})$ nanofluids flow inside a circular tube is studied numerically. The top half of the tube is heated with constant heat flux while the bottom is insulated. Based on the presented results, the following conclusions can be drawn:

- Between 40% and 50% of concentration of EG, the average heat transfer coefficient has highest values. This coefficient increases when the nanoparticle volume fraction and Reynolds number increase.
- The average Nusselt number of nanofluids with W-EG base fluids is found to be higher than that of water based nanofluids and lower than EG based nanofluids.
- The average heat transfer coefficient ratio (h_{nf}/h_{bf}) increases when the volume fraction of nanoparticles increases. However, from 60% of concentration of EG, these ratios decrease with the increase of the Reynolds number.
- The use of the nanofluids $\text{Al}_2\text{O}_3/(\text{W-EG})$ and $\text{CuO}/(\text{W-EG})$ is unfavorable compared to the use of pure water or water-EG base fluids, but its use is favorable compared to the use of pure EG, except at higher concentration of EG and some volume fractions of nanoparticles.

REFERENCES

- [1] S. Allahyari, A. Behzadmehr, S. M. Hosseini Sarvari, "Conjugate heat transfer of laminar mixed convection of a nanofluid through a horizontal tube with circumferentially non-uniform heating", International Journal of Thermal Sciences, Vol. 50, pp. 1963-1972, 2011
- [2] S. U. S. Choi, "Enhancing thermal conductivity of fluids with nanoparticles", International Mechanical Engineering Congress and Exposition, New York, 1995
- [3] Y. Xuan, Q. Li, "Heat transfer enhancement of nanofluids", International Journal of Heat and Fluid Flow, Vol. 21, pp. 58-64, 2000
- [4] S. Zeinali Heris, S. G. Etemad, M. Nasr Esfahany, "Experimental investigation of oxide nanofluids laminar flow convective heat transfer", International Communications in Heat and Mass Transfer, Vol. 33, No. 4, pp. 529-535, 2006
- [5] E. Ahmed, H. A. Mohammed, M. Z. Yusoff, "Heat transfer enhancement of laminar nanofluids flow in a triangular duct using vortex generator", Superlattices and Microstructures, Vol. 52, pp. 398-415, 2012
- [6] W. Yu, H. Xie, Y. Li, L. Chen, Q. Wang, "Experimental investigation on the heat transfer properties of Al_2O_3 nanofluids using the mixture of ethylene glycol and water as base fluid", Powder Technology, Vol. 230, pp. 14-19, 2012
- [7] R. Strandberg, D. K. Das, "Finned tube performance evaluation with nanofluids and conventional heat transfer fluids", International Journal of Thermal Sciences, Vol. 49, pp. 580-588, 2010
- [8] R. S. Vajjha, D. K. Das, "Experimental determination of thermal conductivity of three nanofluids and development of new correlations", International Journal of Heat and Mass Transfer, Vol. 52, pp. 4675-4682, 2009
- [9] R. S. Vajjha, D. K. Das, B. M. Mahagaonkar, "Density Measurement of Different Nanofluids and Their Comparison with Theory", Petroleum Science and Technology, Vol. 27, pp. 612-624, 2009
- [10] V. Kumaresan, R. Velraj, "Experimental investigation of the thermo-physical properties of water-ethylene glycol mixture based CNT nanofluids", Thermochimica Acta, Vol. 545, pp. 180-186, 2012
- [11] L. S. Sundar, M. K. Singh, E. V. Ramana, B. Singh, J. Gracio, A. C. M. Sousa, "Enhanced Thermal Conductivity and Viscosity of Nanodiamond-Nickel Nanocomposite Nanofluids", Scientific Reports, Vol. 4, Art. No. 4039, 2014
- [12] R. S. Vajjha, D. K. Das, "Specific Heat Measurement of Three Nanofluids and Development of New Correlations", Journal of Heat Transfer, Vol. 131, No. 7, Art. No. 071601, 2009
- [13] R. S. Vajjha, D. K. Das, D. P. Kulkarni, "Development of new correlations for convective heat transfer and friction factor in turbulent regime for nanofluids", International Journal of Heat and Mass Transfer, Vol. 53, pp. 4607-4618, 2010
- [14] M. S. Mojarrad, A. Keshavarz, M. Ziabasharagh, M. Mehdi, "Experimental investigation on heat transfer enhancement of alumina/water and alumina/water-ethylene glycol nanofluids in thermally developing laminar flow", Experimental Thermal and Fluid Science, Vol. 53, pp. 111-118, 2014
- [15] M. M. Sarafraz, F. Hormozi, "Intensification of forced convection heat transfer using biological nanofluid in a double-pipe heat exchanger", Experimental Thermal and Fluid Science, Vol. 66, pp. 279-289, 2015
- [16] B. A. Bhanvase, M. R. Sarode, L. A. Putterwar, K. A. Abdullah, M. P. Deosarkar, S. H. Sonawane, "Intensification of convective heat transfer in water/ethylene glycol based nanofluids containing TiO_2 nanoparticles", Chemical Engineering and Processing, Vol. 82, pp. 123-131, 2014
- [17] V. Kumaresan, R. Velraj, S. K. Das, "Convective heat transfer characteristics of secondary refrigerant based CNT nanofluids in a tubular heat exchanger", International Journal of Refrigeration, Vol. 35, pp. 2287-2296, 2012
- [18] V. Kumaresan, S. Mohaideen Abdul Khader, S. Karthikeyan, R. Velraj, "Convective heat transfer characteristics of CNT nanofluids in a tubular heat exchanger of various lengths for energy efficient cooling/heating system", International Journal of Heat and Mass Transfer, Vol. 60, pp. 413-421, 2013
- [19] E. Abu-Nada, A. J. Chamkha, "Effect of nanofluid variable properties on natural convection in enclosures filled with a CuO-EG-Water nanofluid", International Journal of Thermal Sciences, Vol. 49, pp. 2339-2352, 2010
- [20] B. C. Pak, Y. I. Cho, "Hydrodynamic and heat transfer study of dispersed fluids with submicron metallic oxide particles", Experimental Heat Transfer, Vol. 11, pp. 151-170, 1998

- [21] Y. Xuana, W. Roetzel, "Conceptions for heat transfer correlation of nanofluids", International Journal of Heat and Mass Transfer, Vol. 43, pp. 3701-3707, 2000
- [22] H. A. Mohammed, A. N. Al-Shamani, J. M. Sheriff, "Thermal and hydraulic characteristics of turbulent nanofluids flow in a rib-groove channel", International Communications in Heat and Mass Transfer, Vol. 39, pp. 1584-1594, 2012
- [23] R. S. Vajjha, D. K. Das, "A review and analysis on influence of temperature and concentration of nanofluids on thermophysical properties, heat transfer and pumping power", International Journal of Heat and Mass Transfer, Vol. 55, pp. 4063-4078, 2012
- [24] E. Esmaeilzadeh, H. Almohammadi, S. Nasiri Vatan, A. N. Omrani "Experimental investigation of hydrodynamics and heat transfer characteristics of γ -Al₂O₃/water under laminar flow inside a horizontal tube", International Journal of Thermal Sciences, Vol. 63, pp. 361-37, 2013
- [25] S. Suresh, K. P. Venkitaraj, P. Selvakumar, M. Chandrasekar, "Effect of Al₂O₃-Cu/water hybrid nanofluid in heat transfer", Experimental Thermal and Fluid Science, Vol. 38, pp. 54-60, 2012
- [26] P. Razi, M. A. Akhavan-Behabadi, M. Saeedinia, "Pressure drop and thermal characteristics of CuO-base oil nanofluid laminar flow in flattened tubes under constant heat flux", International Communications in Heat and Mass Transfer, Vol. 38, pp. 964-971, 2011
- [27] F. P. Incropera, D. P. De Witt, T. Bergman, A. Lavine, Fundamentals of heat and mass transfer, Wiley, 2006
- [28] A. Bejan, A. D. Kraus, Heat Transfer Handbook, John Wiley & Sons, 2003